Journal of Biomedical Optics

BiomedicalOptics.SPIEDigitalLibrary.org

Theoretical model of blood flow measurement by diffuse correlation spectroscopy

Sava Sakadžić
David A. Boas
Stefan A. Carp

SPIE.

Sava Sakadžić, David A. Boas, Stefan A. Carp, "Theoretical model of blood flow measurement by diffuse correlation spectroscopy," *J. Biomed. Opt.* **22**(2), 027006 (2017), doi: 10.1117/1.JBO.22.2.027006.

Journal of Biomedical Optics 22(2), 027006 (February 2017)

Theoretical model of blood flow measurement by diffuse correlation spectroscopy

Sava Sakadžić,* David A. Boas, and Stefan A. Carp
Massachusetts General Hospital and Harvard Medical School, Optics Division, Athinoula A. Martinos Center for Biomedical Imaging, Department of Radiology, Charlestown, Massachusetts, United States

Abstract. Diffuse correlation spectroscopy (DCS) is a noninvasive method to quantify tissue perfusion from measurements of the intensity temporal autocorrelation function of diffusely scattered light. However, DCS autocorrelation function measurements in tissue better match theoretical predictions based on the diffusive motion of the scatterers than those based on a model where the advective nature of blood flow dominates the stochastic properties of the scattered light. We have recently shown using Monte Carlo (MC) simulations and assuming a simplistic vascular geometry and laminar flow profile that the diffusive nature of the DCS autocorrelation function decay is likely a result of the shear-induced diffusion of the red blood cells. Here, we provide theoretical derivations supporting and generalizing the previous MC results. Based on the theory of diffusing-wave spectroscopy, we derive an expression for the autocorrelation function along the photon path through a vessel that takes into account both diffusive and advective scatterer motion, and we provide the solution for the DCS autocorrelation function in a semi-infinite geometry. We also derive the correlation diffusion and correlation transfer equation, which can be applied for an arbitrary sample geometry. Further, we propose a method to take into account realistic vascular morphology and flow profile. [DOI: 10.1117/1.JBO.22.2.027006]

Keywords: diffuse correlation spectroscopy; diffusing-wave spectroscopy; scattering; random media; autocorrelation function; blood flow; correlation transfer equation; correlation diffusion equation.

Paper 160850R received Dec. 12, 2016; accepted for publication Jan. 30, 2017; published online Feb. 24, 2017.

1 Introduction

Diffuse correlation spectroscopy (DCS) is a method for measuring blood flow based on diffusing-wave spectroscopy (DWS) in heterogeneous multiple-scattering media.[1,2] By measuring the intensity fluctuations of light diffusely reflected from tissue, DCS offers a measure of microvascular blood flow and has been successfully validated against other blood flow measurement techniques, such as arterial spin labeling, magnetic resonance imaging,[3–6] Doppler ultrasound,[7,8] xenon-enhanced computed tomography,[9] and fluorescent microspheres.[10]

The analysis of the DCS signal obtained in the validation studies cited above implies that diffusion-like red blood cell (RBC) motion largely defines the shape of the intensity autocorrelation function, while the effect of the advective (sometimes referred to as convective) RBC motion is significantly smaller.[11,12] Lacking a first principles-based understanding of the nature of the measured signal, DCS has been employed to provide a "blood flow index" obtained by fitting the intensity autocorrelation decay for the RBC "diffusion coefficient," which has been shown to correlate well with the relative changes in blood flow as mentioned above.

Recent articles have indicated that shear-induced diffusive RBC motion may contribute to the DCS signal,[12,13] providing a possible mechanistic explanation for the observed diffusion-like RBC motion in the decay of the intensity autocorrelation function. Here, we provide a theoretical model for the DCS signal based on DWS that includes both advective RBC motion along the blood vessels and shear-induced RBC diffusion. In a recent article, we have shown using Monte Carlo (MC) simulations and assuming a simplistic vascular geometry and laminar flow profile that the diffusive nature of the decay of the DCS autocorrelation function is likely the result of the shear-induced diffusion experienced by RBC during vascular transport.[14] Here, we provide theoretical derivations supporting and generalizing the previous MC results. We derive expressions for the autocorrelation function along the photon path that take into account both diffusive and advective motions of the scattering particles and provide the solution for the DCS autocorrelation function in a semi-infinite geometry. Our model predicts that for all source–detector separations commonly applied in DCS measurements, the DCS signal is, as expected, dominated by the shear-induced RBC diffusion. We also provide an expression for the DCS signal in a realistic vascular network with a heterogeneous distribution of vessels with different diameters and average blood flows. Finally, we derive the expressions for the correlation transfer equation (CTE) and correlation diffusion equation (CDE), which can be used to model the DCS signal in tissue with a complex geometry and heterogeneous blood flow distribution.

2 Phase Accumulation in a Vessel

In this section, we consider the optical phase accumulation along the scattering path through a single blood vessel. We assume that a partial wave scatters first from a scatterer at location $\mathbf{r}_0$ outside the vessel, then experiences N consecutive scattering events from RBCs located at $\mathbf{r}_1, \cdots \mathbf{r}_N$ inside the

*Address all correspondence to: Sava Sakadžić, E-mail: sava.sakadzic@mgh.harvard.edu

vessel, and finally exits the vessel scattering at location $\mathbf{r}_{N+1}$ outside the vessel. The accumulated optical phase $\phi(t)$ along this path is given as

$$\phi(t) = \sum_{i=1}^{N+1} k_0 n |\mathbf{r}_i(t) - \mathbf{r}_{i-1}(t)|, \tag{1}$$

where n is an optical index of refraction, $k_0 = 2\pi/\lambda_0$, λ_0 is the wavelength of light in a vacuum, and $|\mathbf{r}|$ represents the vector magnitude. Equation (1) can be approximated as

$$\phi(t) \approx \sum_{i=1}^{N+1} k_0 n l_{i,0} + \sum_{i=1}^{N+1} k_0 n \hat{\mathbf{\Omega}}_i \cdot [\Delta\mathbf{r}_i(t) - \Delta\mathbf{r}_{i-1}(t)], \tag{2}$$

where $\hat{\mathbf{\Omega}}_i = (\mathbf{r}_{i,0} - \mathbf{r}_{i-1,0})/l_{i,0}$, $\mathbf{r}_{i,0}$ is i'th scatterer position at $t = 0$, $l_{i,0} = |\mathbf{r}_{i,0} - \mathbf{r}_{i-1,0}|$, $\mathbf{r}_i(t) = \mathbf{r}_{i,0} + \Delta\mathbf{r}_i(t)$, and $\Delta\mathbf{r}_i(t)$ is a small displacement of the i'th scatterer at time t with respect to its original position $\mathbf{r}_{i,0}$. If we further assume that only scatterers inside the vessel exhibit motion [i.e., $\Delta\mathbf{r}_0(t) = 0$ and $\Delta\mathbf{r}_{N+1}(t) = 0$], then it follows from Eq. (2) that the difference of the accumulated phase $\Delta\phi(t,\tau) = \phi(t+\tau) - \phi(t)$ is given as

$$\Delta\phi(t,\tau) = k_0 n_0 \sum_{i=1}^{N} \Delta\mathbf{r}_i(t,\tau) \cdot (\hat{\mathbf{\Omega}}_i - \hat{\mathbf{\Omega}}_{i+1}), \tag{3}$$

where $\Delta\mathbf{r}_i(t,\tau) = \Delta\mathbf{r}_i(t+\tau) - \Delta\mathbf{r}_i(t)$.

The temporal electric field (E) autocorrelation function $g_1(\tau)$ is computed as $g_1(\tau) = \langle E(t)E^*(t+\tau)\rangle = \langle \exp[-i\Delta\phi(t,\tau)]\rangle$, where $\langle\rangle$ represents an ensemble average and i is the imaginary unit. In the case of a small phase difference term $\Delta\phi(t,\tau)$, the autocorrelation function can be approximated as $g_1(\tau) \approx \exp[-\frac{1}{2}F(\tau)]$, where $F(\tau) = \langle \Delta\phi^2(t,\tau)\rangle$.

To compute $F(\tau)$, we first assume that $\Delta\mathbf{r}_i(t,\tau)$ in the vessel can be expressed as

$$\Delta\mathbf{r}_i(t,\tau) = \Delta\mathbf{r}_{i,\mathrm{D}}(\tau) + \mathbf{v}_i\tau, \tag{4}$$

where $\mathbf{v}_i$ represents a laminar RBC velocity of the i'th scatterer and $\Delta\mathbf{r}_{i,\mathrm{D}}(t,\tau)$ accounts for the diffusive RBC motion due to shear flow. We can now express $F(\tau)$ as

$$F(\tau) = F_{\mathrm{D}}(\tau) + F_{\mathrm{V}}(\tau) + F_{\mathrm{D,V}}(\tau), \tag{5}$$

where a diffusion term $F_{\mathrm{D}}(\tau)$ is given as

$$F_{\mathrm{D}}(\tau) = k_0^2 n^2 \left\langle \left[\sum_{i=1}^{N} \Delta\mathbf{r}_{i,\mathrm{D}}(\tau) \cdot (\hat{\mathbf{\Omega}}_i - \hat{\mathbf{\Omega}}_{i+1}) \right]^2 \right\rangle, \tag{6}$$

a velocity term $F_{\mathrm{V}}(\tau)$ is given as

$$F_{\mathrm{V}}(\tau) = k_0^2 n^2 \left\langle \left[\sum_{i=1}^{N} \tau\mathbf{v}_i \cdot (\hat{\mathbf{\Omega}}_i - \hat{\mathbf{\Omega}}_{i+1}) \right]^2 \right\rangle, \tag{7}$$

and a mixed term $F_{\mathrm{D,V}}(\tau)$ is given as

$$F_{\mathrm{D,V}}(\tau) = k_0^2 n^2 \left\langle 2 \left[\sum_{i=1}^{N} \Delta\mathbf{r}_{i,\mathrm{D}}(\tau) \cdot (\hat{\mathbf{\Omega}}_i - \hat{\mathbf{\Omega}}_{i+1}) \right] \times \left[\sum_{j=1}^{N} \tau\mathbf{v}_j \cdot (\hat{\mathbf{\Omega}}_j - \hat{\mathbf{\Omega}}_{j+1}) \right] \right\rangle. \tag{8}$$

Due to isotropic diffusive motion, the diffusive and advective motions are uncorrelated; thus, the mixed term $F_{\mathrm{D,V}}(\tau) = 0$.

2.1 *Diffusion Term*

To compute the ensemble average in Eq. (6), we first consider that the probability density function for diffusive RBC motion can be approximated as[15]

$$P[\Delta\mathbf{r}_{i,\mathrm{D}}(\tau)] = \frac{1}{(4\pi D_i\tau)^{3/2}} \exp\left[-\frac{|\Delta\mathbf{r}_{i,\mathrm{D}}(\tau)|^2}{4D_i\tau}\right], \tag{9}$$

where D_i is the RBC diffusion coefficient due to the shear flow at location $\mathbf{r}_{i,0}$. Since the diffusive displacements $\Delta\mathbf{r}_{i,\mathrm{D}}(\tau)$ and $\Delta\mathbf{r}_{j,\mathrm{D}}(\tau)$ of RBCs involved in consecutive scattering events are uncorrelated, Eq. (6) can be reduced to

$$F_{\mathrm{D}}(\tau) = k_0^2 n^2 \sum_{i=1}^{N} \langle |\Delta\mathbf{r}_{i,\mathrm{D}}(\tau) \cdot (\hat{\mathbf{\Omega}}_i - \hat{\mathbf{\Omega}}_{i+1})|^2 \rangle. \tag{10}$$

The ensemble average on the right side of Eq. (10) can be calculated as

$$\begin{aligned} \langle |\Delta\mathbf{r}_{i,\mathrm{D}}(\tau)(\hat{\mathbf{\Omega}}_i - \hat{\mathbf{\Omega}}_{i+1})|^2 \rangle &= \frac{4}{3}\pi \langle |\hat{\mathbf{\Omega}}_i - \hat{\mathbf{\Omega}}_{i+1}|^2 \rangle \\ &\times \int_0^{+\infty} P(|\Delta\mathbf{r}_{i,\mathrm{D}}|)|\Delta\mathbf{r}_{i,\mathrm{D}}|^4 d|\Delta\mathbf{r}_{i,\mathrm{D}}| \\ &= 4(1-g)D_i\tau, \end{aligned} \tag{11}$$

where $g = \langle \hat{\mathbf{\Omega}}_i \cdot \hat{\mathbf{\Omega}}_{i+1} \rangle$ is a scattering anisotropy coefficient. Equation (10) can be subsequently written as

$$F_{\mathrm{D}}(\tau) = k_0^2 n^2 4(1-g)\tau \sum_{i=1}^{N} D_i, \tag{12}$$

which is a generalized form of the well-known equation for the autocorrelation phase term for multiple scattering in the case of Brownian motion in a uniform medium

$$F_{D_B}(\tau) = \frac{k_0^2 n^2 4 D_{\mathrm{B}} \tau s}{l_{\mathrm{tr}}}, \tag{13}$$

where D_{B} is the diffusion coefficient for Brownian motion, s is the path length of light, and l_{tr} is the transport mean free path. Note that the path length of light, s, divided by l_{tr} is the average number of "isotropic" photon random walk steps (N_{tr}), which is related to the number of scattering events by $N_{\mathrm{tr}} = (1-g)N$.

2.2 *Velocity Term*

The anisotropy factor g for light scattering from RBCs is quite high ($g > 0.95$[16]). This implies that the phase increments along the scattering path through the vessel are correlated, which makes calculation of the velocity term expressed by Eq. (7) more complex. We will start the calculation by assuming without loss of generality that the vessel axis is parallel with the Z-axis such that velocities $\mathbf{v}_i$ can be expressed as $\mathbf{v}_i = v_i\hat{\mathbf{\Omega}}_z$, where $\hat{\mathbf{\Omega}}_z$ is a unit vector along the Z-axis. We can thus write Eq. (7) as

$$F_{\mathrm{V}}(\tau)=k_0^2n^2\tau^2\sum_{i=1}^{N}v_i^2\langle(x_i-x_{i+1})^2\rangle + k_0^2n^2\tau^2\sum_{i=2}^{N}\sum_{j=1}^{i-1}v_iv_j\langle(x_i-x_{i+1})(x_j-x_{j+1})\rangle, \quad (14)$$

where $x_i=\hat{\mathbf{\Omega}}_z\cdot\hat{\mathbf{\Omega}}_i$. To calculate the ensemble averages in the above equation, we will follow the procedure outlined in Sakadžić and Wang.[17] We assume that the probability of a random walk $p(\mathbf{l}_1,\ldots,\mathbf{l}_N)$ through the vessel can be expressed as

$$p(\mathbf{l}_1,\ldots,\mathbf{l}_{N+1})=f^{(N+1)}(\cos\,\theta_1,\ldots,\cos\,\theta_{N+1})\prod_{j=1}^{N+1}p(l_j), \quad (15)$$

where $\mathbf{l}_i=l_i\hat{\mathbf{\Omega}}_i$ is the vector given by the free path between scatterers $i-1$ and i (i.e., $\mathbf{l}_i=\mathbf{r}_i-\mathbf{r}_{i-1}$), $p(l_i)=\mu_{\mathrm{s}}\exp(-\mu_{\mathrm{s}}l_i)$ is the probability density of the free path l_i, μ_{s} is the scattering coefficient, and $f^{(N+1)}(\cos\,\theta_1,\ldots,\cos\,\theta_{N+1})$ is the probability density function that the scattering path follows a Markov chain of scattering angles $\theta_1,\ldots,\theta_{N+1}$. $f^{(N+1)}()$ can be further represented as

$$f^{(N+1)}(\cos\,\theta_1,\ldots,\cos\,\theta_{N+1})=\tilde{p}_{\mathrm{s}}(\cos\,\theta_1)\prod_{j=1}^{N}f^{(2)}(\cos\,\theta_j,\cos\,\theta_{j+1}), \quad (16)$$

where $\tilde{p}_{\mathrm{s}}(\cos\,\theta_1)$ is the probability of the initial photon direction conveniently set to 0.5. $f^{(2)}(\cos\,\theta_j,\cos\,\theta_{j+1})$ is thus given as

$$f^{(2)}(\cos\theta_j,\cos\theta_{j+1})=\sum_{m=0}^{+\infty}\frac{2m+1}{2}g_mP_m(\cos\theta_j)P_m(\cos\theta_{j+1}), \quad (17)$$

where g_m is the m'th moment of the scattering phase function and $P_m(\cos\,\theta)$ is a Legendre polynomial. We further assume that scattering angles can be described by the Henyey–Greenstein phase function (i.e., $g_m=g^m$). By following the derivations from Sakadžić and Wang,[17] one can show that $\langle x_i^2\rangle=1/3$ and $\langle x_ix_{i+n}\rangle=g^n/3$. Therefore, Eq. (14) can be expressed as

$$F_{\mathrm{V}}(\tau)=k_0^2n^2\tau^2\frac{2}{3}(1-g)\sum_{i=1}^{N}v_i^2 - k_0^2n^2\tau^2\frac{2}{3}(1-g)^2\sum_{i=2}^{N}\sum_{j=1}^{i-1}v_iv_jg^{i-j-1}. \quad (18)$$

2.3 *Approximate Solution*

If we make several assumptions that are consistent with realistic soft biological tissue properties, we can significantly simplify the expressions for $F_{\mathrm{D}}(\tau)$ and $F_{\mathrm{V}}(\tau)$. We first assume that absorption inside the vessel has a negligible influence on the radiance distribution, which is expected given that the absorption length in blood is ~2 to 4 mm at the optical wavelengths in the 780- to 850-nm range typically used in DCS measurements.[16] Next, we assume that both the measured tissue volume and the partial volume of blood are large such that light propagation is diffusive, that vessels are penetrated by photons from a sufficient number of angles to reproduce the ensemble averaging in our calculations, and that multiple scattering within larger vessels results in effective sampling of all radial locations. Under such conditions, photons have an equal probability of scattering from each location inside the vessel, and the location-specific terms v_i and D_i can be replaced by their average values, as we observed and documented in our previous MC-based study.[14] If we know the vessel radius R and the intravascular radial distributions of the RBC velocity $v(r_i)$ and diffusion coefficient $D(r_i)$, we may write

$$F_{\mathrm{D}}(\tau)=4k_0^2n^2(1-g)ND_{\mathrm{av}}\tau, \quad (19)$$

$$F_{\mathrm{V}}(\tau)=\frac{2}{3}k_0^2n^2(1-g^N)v_{\mathrm{av}}^2\tau^2, \quad (20)$$

where

$$D_{\mathrm{av}}=\frac{2}{R^2}\int_0^R D(r)r\mathrm{d}r, \quad (21)$$

and

$$v_{\mathrm{av}}=\frac{2}{R^2}\int_0^R v(r)r\mathrm{d}r \quad (22)$$

are the average values of D_i and v_i.

We can introduce another approximation when g is close to 1, which is typically the case with scattering from the RBCs: $1-g^N\approx(1-g)N$. For example, for $(g=0.95;N<4)$ the relative error of this approximation is <5%. We can finally write

$$F_{\mathrm{D}}(\tau)=4k_0^2n^2sl_{\mathrm{tr}}^{-1}D_{\mathrm{av}}\tau, \quad (23)$$

$$F_{\mathrm{V}}(\tau)=\frac{2}{3}k_0^2n^2sl_{\mathrm{tr}}^{-1}v_{\mathrm{av}}^2\tau^2, \quad (24)$$

where $(1-g)N\approx s/l_{\mathrm{tr}}$ and s is the photon path length through the vessel.

3 Realistic Vascular Morphology

So far we have developed the expression for the autocorrelation function $g_1(\tau)$ for a path length s through a single vessel

$$g_1(\tau)=\exp\left[-\frac{1}{2}F(\tau)\right], \quad (25)$$

where $F(\tau)=F_{\mathrm{D}}(\tau)+F_{\mathrm{V}}(\tau)$ and terms $F_{\mathrm{D}}(\tau)$ and $F_{\mathrm{V}}(\tau)$ are given by Eqs. (23) and (24), respectively.

In a realistic soft biological tissue, such as the brain cortex, vessels of different diameters and average RBC velocities will be present. We may first associate each vessel with the arterial, venous, or capillary compartment. Each of these compartments contains a population of vessels with different diameters and average RBC velocities. For a path length s sufficiently long through the tissue to probe all of these vessel types, we can write

$$F(\tau)=F_{\mathrm{art}}(\tau)+F_{\mathrm{vein}}(\tau)+F_{\mathrm{cap}}(\tau)+F_{\mathrm{tiss}}(\tau), \quad (26)$$

where $F_{\mathrm{art}}(\tau)$, $F_{\mathrm{vein}}(\tau)$, $F_{\mathrm{cap}}(\tau)$, and $F_{\mathrm{tiss}}(\tau)$ represent contributions from arterial, venous, capillary, and extravascular (i.e., tissue) compartments, respectively. They can be expressed as

$$F_{\text{art}}(\tau) = k_0^2 n^2 s l_{\text{tr,vasc}}^{-1} \int_{R_{\text{art,min}}}^{R_{\text{art,max}}} \delta_{\text{art}}(R)\mathrm{d}R \times \left\{ 4D_{\text{av}}[R, v_{\text{art,av}}(R)]\tau + \frac{2}{3} v_{\text{art,av}}^2(R)\tau^2 \right\}, \quad (27)$$

$$F_{\text{vein}}(\tau) = k_0^2 n^2 s l_{\text{tr,vasc}}^{-1} \int_{R_{\text{vein,min}}}^{R_{\text{vein,max}}} \delta_{\text{vein}}(R)\mathrm{d}R \times \left\{ 4D_{\text{av}}[R, v_{\text{vein,av}}(R)]\tau + \frac{2}{3} v_{\text{vein,av}}^2(R)\tau^2 \right\}, \quad (28)$$

$$F_{\text{cap}}(\tau) = k_0^2 n^2 s l_{\text{tr,vasc}}^{-1} \delta_{\text{cap}} \int_{v_{\text{cap,min}}}^{v_{\text{cap,max}}} p_{\text{cap}}(v_{\text{cap}}) dv_{\text{cap}} \times \left[4D_{\text{av}}(v_{\text{cap}})\tau + \frac{2}{3} v_{\text{cap}}^2 \tau^2 \right], \quad (29)$$

and

$$F_{\text{tiss}}(\tau) = k_0^2 n^2 s l_{\text{tr,tiss}}^{-1} \delta_{\text{tiss}} 4D_{\text{B}}\tau, \quad (30)$$

where $l_{\text{tr,tiss}}$ is the transport mean free path in tissue. We assumed that hematocrit is constant and that the transport mean free path $l_{\text{tr,vasc}}$ in the vasculature is the same in all vessels. δ_{tiss} and δ_{cap} are volume fractions of the tissue and capillary compartments, respectively. $\delta_{\text{art}}(R)$ and $\delta_{\text{vein}}(R)$ are the densities of the volume fraction of arteries and veins with radius R, respectively. For simplicity, we neglected the radial differences between capillaries and considered only their velocity distribution $p_{\text{cap}}(v_{\text{cap}})$. We also neglected any potential velocity distributions in arteries and veins with the same radius and assumed that the average velocity in these vessels can be represented as a function of the vessel radius [in general, $v_{\text{art,av}}(R) \neq v_{\text{vein,av}}(R)$]. Finally, only Brownian motion characterized by the diffusion constant D_{B} is considered in tissue.

Based on Eqs. (27)–(30), we need a detailed knowledge of the vascular morphology, RBC rheology, and D_{B} in tissue to compute $F_{\text{art}}(\tau)$, $F_{\text{vein}}(\tau)$, $F_{\text{cap}}(\tau)$, and $F_{\text{tiss}}(\tau)$. This information is not readily accessible, but it may be available in the near future due to the current progress in experimental techniques.[18] Another factor to consider is how much our model of diffusive RBC motion departs from reality in vessels with a small diameter (<10 μm), which include capillaries, precapillary arterioles, and postcapillary venules. Further measurements and numerical modelings of the microvascular blood flow and morphology may inform modifications of Eqs. (27)–(30) to better represent microvascular compartments.

In the following sections, we will show that some important relations between the DCS measurements and blood flow can already be deduced from Eqs. (27)–(30).

4 Correlation Transfer and Diffusion Equations

We start with an integral form of the CTE for scatterers experiencing diffusive, linear, or oscillatory motion[19–21]

$$I(\mathbf{r}, \hat{\mathbf{\Omega}}, \tau) = I_0(\mathbf{r}, \hat{\mathbf{\Omega}}, \tau) + \int_{\mathbf{r}_0}^{\mathbf{r}} \mu_{\text{s}}(\mathbf{r}_s) e^{-\mu_{\text{t}}(\mathbf{r}_{\text{s}})|\mathbf{r}_{\text{s}} - \mathbf{r}_0|} \times \int_{4\pi} p(\hat{\mathbf{\Omega}}, \hat{\mathbf{\Omega}}') \langle e^{-iK_{\text{r}}(\mathbf{r}_{\text{s}})(\hat{\Omega} - \hat{\Omega}')\cdot\Delta\mathbf{r}_{\text{s}}(\tau)} \rangle \times I(\mathbf{r}_{\text{s}}, \hat{\mathbf{\Omega}}', \tau) d|\mathbf{r}_{\text{s}} - \mathbf{r}_0| \mathrm{d}\mathbf{\Omega}', \quad (31)$$

where $I(\mathbf{r}, \hat{\mathbf{\Omega}}, \tau)$ is the time-varying-specific intensity at position $\mathbf{r}$ and in direction given by the unity vector $\hat{\mathbf{\Omega}}$. $I(\mathbf{r}, \hat{\mathbf{\Omega}}, \tau)$ represents an angular spectrum of the mutual coherence function, and it should be noted that the temporal field correlation function can be obtained as an integral of $I(\mathbf{r}, \hat{\mathbf{\Omega}}, \tau)$ over all solid angles Ω. $I_0(\mathbf{r}, \hat{\mathbf{\Omega}}, \tau)$ is the unscattered (coherent) time-varying-specific intensity originating from the point $\mathbf{r}_0$ at the boundary. The integral on the right side of the equation represents contributions of time-varying-specific intensities $I(\mathbf{r}_{\text{s}}, \hat{\mathbf{\Omega}}', \tau)$ from directions $\hat{\mathbf{\Omega}}'$ scattered into direction $\hat{\mathbf{\Omega}}$ along the path from $\mathbf{r}_0$ to $\mathbf{r}$ at locations $\mathbf{r}_s$. $p(\hat{\mathbf{\Omega}}, \hat{\mathbf{\Omega}}')$ is a scattering phase function describing the probability of scattering from $\hat{\mathbf{\Omega}}'$ into $\hat{\mathbf{\Omega}}$ direction. We emphasize that scattering coefficient $\mu_{\text{s}}(\mathbf{r})$ and extinction coefficient $\mu_{\text{t}}(\mathbf{r})$ are functions of position $\mathbf{r}$ in the inhomogeneous scattering medium. Finally, $\langle \exp[-iK_{\text{r}}(\mathbf{r}_{\text{s}})(\hat{\mathbf{\Omega}} - \hat{\mathbf{\Omega}}') \cdot \Delta\mathbf{r}_{\text{s}}(\tau)] \rangle$ is the decorrelation contribution from the scatterer displacement $\Delta\mathbf{r}_{\text{s}}(\tau)$ due to both diffusive and advective (linear) motion, where $\langle\rangle$ stands for the ensemble average. K_{r} is given by $K_{\text{r}}(\mathbf{r}) = k_0 n + 2\pi \text{Re}[f(\hat{\mathbf{\Omega}}, \hat{\mathbf{\Omega}})]\rho_{\text{s}}(\mathbf{r})/(k_0 n)$, where the second term on the right side accounts for the reduction of the propagation speed of the mean field due to multiple wave scattering, $\rho_{\text{s}}(\mathbf{r})$ is the density of scatterers, $f(\hat{\mathbf{\Omega}}_{\text{sc}}, \hat{\mathbf{\Omega}}_{\text{inc}})$ is the optical scattering amplitude from direction $\hat{\mathbf{\Omega}}_{\text{inc}}$ into direction $\hat{\mathbf{\Omega}}_{\text{sc}}$, and Re[] stands for the real value.

The scatterer displacement term at location $\mathbf{r}$ can be expressed as $\Delta\mathbf{r}(\tau) = \Delta\mathbf{r}_{\text{D}}(\tau) + \mathbf{v}(\mathbf{r})\tau$, where $\Delta\mathbf{r}_{\text{D}}(\tau)$ is due to either RBC diffusive motion inside the vessel or Brownian motion of scatterers outside the vessel. RBC velocity $\mathbf{v}(\mathbf{r})$ is not zero only inside the vessel. To perform ensemble averaging, we will apply the same approximation from Sec. 2

$$\langle \exp[-iK_{\text{r}}(\mathbf{r}_{\text{s}})(\hat{\mathbf{\Omega}} - \hat{\mathbf{\Omega}}') \cdot \Delta\mathbf{r}_{\text{s}}(\tau)] \rangle = \exp\left[-\frac{1}{2} F(\mathbf{r}_{\text{s}}, \hat{\mathbf{\Omega}} - \hat{\mathbf{\Omega}}', \tau) \right], \quad (32)$$

where

$$F(\mathbf{r}_{\text{s}}, \hat{\mathbf{\Omega}} - \hat{\mathbf{\Omega}}', \tau) = \langle [K_{\text{r}}(\mathbf{r}_{\text{s}})(\hat{\mathbf{\Omega}} - \hat{\mathbf{\Omega}}') \cdot \Delta\mathbf{r}_{\text{s}}(\tau)]^2 \rangle. \quad (33)$$

Following the steps from Sec. 2 (phase accumulation in a vessel), it is easy to show that

$$F(\mathbf{r}_{\text{s}}, \hat{\mathbf{\Omega}} - \hat{\mathbf{\Omega}}', \tau) = K_{\text{r}}^2(\mathbf{r}_{\text{s}})(\hat{\mathbf{\Omega}} - \hat{\mathbf{\Omega}}')^2 2D(\mathbf{r}_{\text{s}})\tau + \text{K}_{\text{r}}^2(\mathbf{r}_{\text{s}})[(\hat{\mathbf{\Omega}} - \hat{\mathbf{\Omega}}') \cdot \mathbf{v}(\mathbf{r}_{\text{s}})]\tau^2. \quad (34)$$

We can now follow the same procedure as in Sakadžić and Wang[21] to convert the integral form of CTE into a differential CTE expression

$$\left(\hat{\mathbf{\Omega}} \frac{\partial}{\partial \mathbf{r}} + \mu_{\text{t}} \right) I(\mathbf{r}, \hat{\mathbf{\Omega}}, \tau) = \mu_{\text{s}} \int_{4\pi} p(\hat{\mathbf{\Omega}}, \hat{\mathbf{\Omega}}') e^{-\frac{1}{2}F(\mathbf{r}, \hat{\mathbf{\Omega}} - \hat{\mathbf{\Omega}}', \tau)} I(\mathbf{r}, \hat{\mathbf{\Omega}}', \tau) \mathrm{d}\mathbf{\Omega}'. \quad (35)$$

We can also allow for the source $S(\mathbf{r}, \hat{\mathbf{\Omega}})$ in the medium and write

$$\left(\hat{\mathbf{\Omega}}\frac{\partial}{\partial \mathbf{r}}+\mu_t\right)I(\mathbf{r},\hat{\mathbf{\Omega}},\tau) = \mu_s\int_{4\pi} p(\hat{\mathbf{\Omega}},\hat{\mathbf{\Omega}}')e^{-\frac{1}{2}F(\mathbf{r},\hat{\mathbf{\Omega}}-\hat{\mathbf{\Omega}}',\tau)}I(\mathbf{r},\hat{\mathbf{\Omega}}',\tau)\mathrm{d}\mathbf{\Omega}' + S(\mathbf{r},\hat{\mathbf{\Omega}}). \tag{36}$$

In the next step, we will derive an expression for the diffusion correlation equation based on this CTE. We first apply the standard approximation

$$I(\mathbf{r},\hat{\mathbf{\Omega}},\tau) = \frac{1}{4\pi}\Phi(\mathbf{r},\tau)+\frac{3}{4\pi}\hat{\mathbf{\Omega}}\cdot\mathbf{J}(\mathbf{r},\tau), \tag{37}$$

where $\Phi(\mathbf{r},\tau)$ is the temporal field autocorrelation function.

We proceed by replacing $I(\mathbf{r},\hat{\mathbf{\Omega}},\tau)$ in Eq. (36) and performing the integral over Ω before and after multiplying Eq. (36) with $\hat{\mathbf{\Omega}}$. To perform the integrations, we apply the following approximation:

$$\exp\left[-\frac{1}{2}F(\mathbf{r},\hat{\mathbf{\Omega}}-\hat{\mathbf{\Omega}}',\tau)\right] \approx 1-\frac{1}{2}F(\mathbf{r},\hat{\mathbf{\Omega}}-\hat{\mathbf{\Omega}}',\tau). \tag{38}$$

This procedure yields the well-known expression for the CDE

$$\nabla[D_s\nabla\Phi(\mathbf{r},\tau)]-[\mu_a+\mu_s'\psi(\mathbf{r},\tau)]\Phi(\mathbf{r},\tau)+S_0(\mathbf{r})=0, \tag{39}$$

where $D_s=(3\mu_s)^{-1}$, $S_0(\mathbf{r})=\int_{4\pi}S(\mathbf{r},\hat{\mathbf{\Omega}})\mathrm{d}\mathbf{\Omega}$, and $\mu_s'\psi(\mathbf{r},\tau)$ is due to the phase difference accumulated along the unit pathlength

$$\mu_s'\psi(\mathbf{r},\tau)=\mu_s'K_r^2 2D_{av}\tau+\mu_s'K_r^2\frac{1}{3}v_{av}^2\tau^2. \tag{40}$$

The average values of the scatterer's diffusion coefficient D_{av} and RBC velocity v_{av} should take into account heterogeneity of the scattering medium on the scale $\sim l_{tr}$, so $\mu_s'\psi(\mathbf{r},\tau)$ should in general be calculated as $s^{-1}[F_{art}(\tau)+F_{vein}(\tau)+F_{cap}(\tau)+F_{tiss}(\tau)]$, where $F_{art}(\tau)$, $F_{vein}(\tau)$, $F_{cap}(\tau)$, and $F_{tiss}(\tau)$ are given by Eqs. (27)–(30).

5 Reflection Geometry

For a scattering medium with the known probability $P(s)$ of a photon path length s between source and detector, we can express the autocorrelation function as

$$G_1(\tau)=\int P(s)\exp\left[-\frac{1}{2}F(\tau)\right]\mathrm{d}s, \tag{41}$$

where the integral is taken over all possible path lengths s.

In DCS, measurements are typically performed in a reflection geometry. For a semi-infinite medium with source–detector separation ρ, diffusion theory provides the analytical expression for the path length probability $P(s)$. If we assume that $F(\tau)$ is linearly proportional to s, such as the case in Eqs. (26)–(30), $G_1(\tau)$ can then be expressed as

$$G_1(\rho,\tau)=G_{1,0}\left[\frac{\exp(-Kr_1)}{r_1}-\frac{\exp(-Kr_2)}{r_2}\right], \tag{42}$$

where

$$K^2=3\mu_a\mu_s'+\frac{2}{3}\mu_s'F^*(\tau), \tag{43}$$

$F^*(\tau)=F(\tau)/s$, $r_1=\sqrt{\rho^2+z_0^2}$, $r_2=\sqrt{\rho^2+(z_0+2z_b)^2}$, $z_0=(\mu_a+\mu_s')^{-1}$, $z_b=\gamma/\mu_s'$, $\gamma=1.76$, and $G_{1,0}$ is scaling constant such that $G_1(\rho,\tau)\to 1$ when $\tau\to 0$.

5.1 *Relative Importance of Diffusive and Advective Red Blood Cell Motions*

We now explore the relative importance of the $F_D(\tau)$ and $F_V(\tau)$ terms. We consider a semi-infinite scattering medium and a DCS measurement in a reflection geometry. For simplicity, we assume $\mu_a=0$, $D_B=0$, and only one vessel type is present in the medium. We further assume that the RBC velocity follows a parabolic radial profile inside the vessel

$$v(r)=V_{max}\left(1-\frac{r^m}{R^m}\right), \tag{44}$$

where $m=2$ and V_{max} is the velocity at the vessel center. From Goldsmith and Marlow,[22] the RBC diffusion coefficient is given by $D(r)=\alpha_{ss}|\partial v(r)/\partial r|$, where α_{ss} (typically around 10^{-6} mm^2) is the shear-induced diffusion coefficient proportionality constant. This allows us to write

$$v_{av}=V_{max}\frac{m}{m+2}, \tag{45}$$

$$D(r)=\alpha_{ss}m\frac{r^{m-1}}{R^m}V_{max}, \tag{46}$$

$$D_{av}=\frac{2m}{m+1}\alpha_{ss}\frac{V_{max}}{R}, \tag{47}$$

$$F^*(\tau)=k_0^2n^2l_{tr}^{-1}\delta_{ves}\left(4D_{av}\tau+\frac{2}{3}v_{av}^2\tau^2\right), \tag{48}$$

where we assumed that $l_{tr}=1$ mm in both the vasculature and the tissue.

Good agreement between Eq. (42) and MC simulations for a similar geometry was already demonstrated by Boas et al.[14] It was shown that for a range of R and V_{max} at $\rho=20$ mm both the advective and, respectively, the diffusive RBC motion contributions to $G_1(\tau)$ can be fit successfully with Eq. (48), providing support for the derivations of the velocity terms in Sec. 2.2. It was also shown that under the same conditions, diffusive RBC motion almost exclusively determines the profile of $G_1(\tau)$. While the summation of diffusive and advective motion terms in Eq. (48) has been considered before,[23] we provided a theoretical support for this assumption that does not assume that uncorrelated optical phase increments accumulated along the path.

Here, we further compare individual contributions of the diffusive and convective RBC motions to the decay of $G_1(\tau)$. Figure 1 shows $G_1(\tau)$ due to $F_D(\tau)$, $F_V(\tau)$, and $F_D(\tau)+F_V(\tau)$ for $V_{max}=2$ mm/s, a vascular volume fraction $\delta_{ves}=2\%$, and a range of vessel radii and source–detector separations. In all cases, term $F_D(\tau)$ strongly dominates the expression for $G_1(\tau)$, in agreement with prior experimental observations[11,12] and our prior MC simulations.[14] While increasing the vessel radius and decreasing the source–detector separation both lead to the

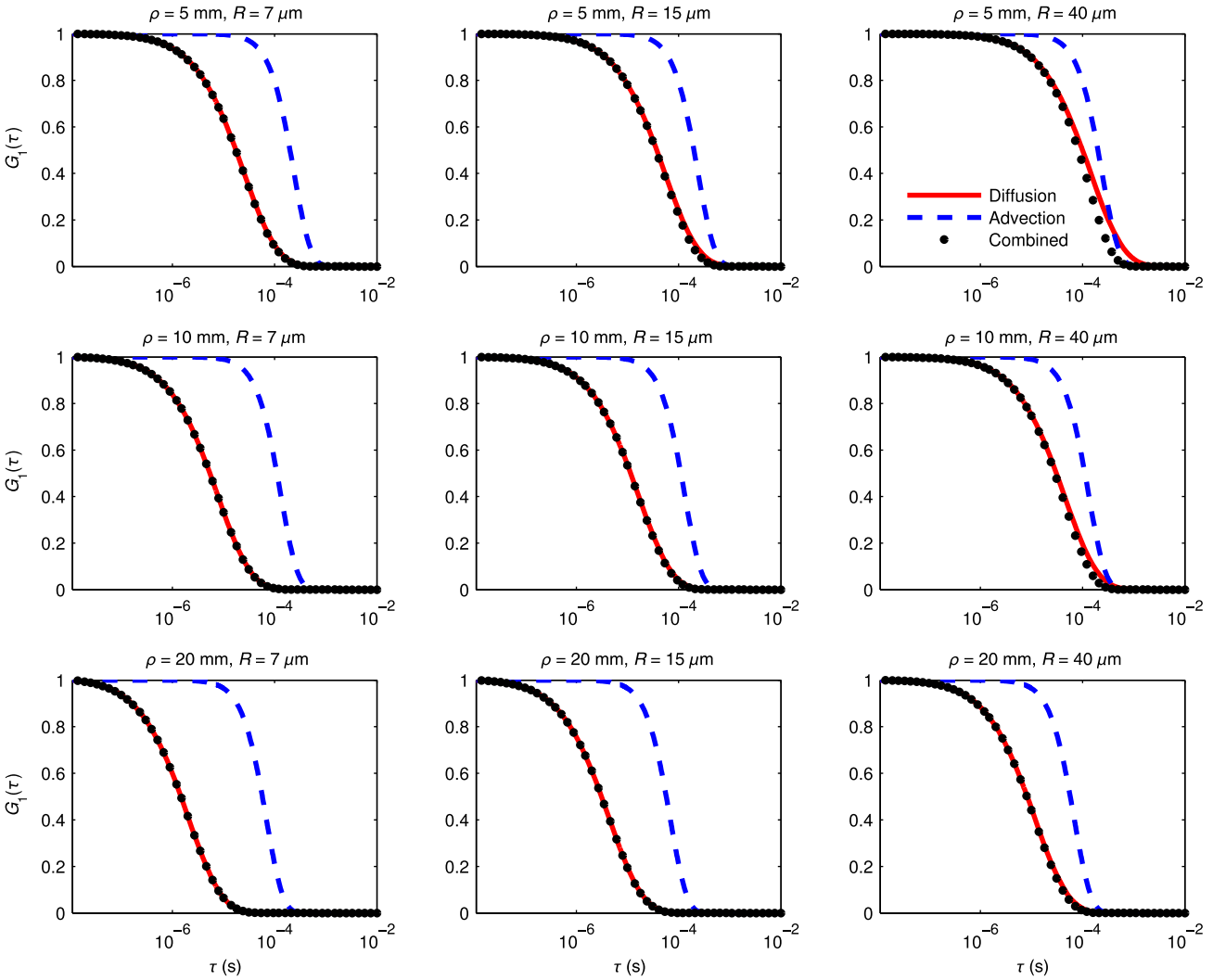

Fig. 1 Comparison of the individual contributions of diffusive RBC motion (red line) and advective RBC motion (blue dashed line) to the total autocorrelation function (black dots) for different values of vessel diameter and source–detector distance.

increased importance of the advective RBC motion, even for the short source–detector separation ($\rho = 5$ mm) and large vessel radius ($R = 40$ μm), $G_1(\tau)$ is still largely determined by the diffusive RBC motion. Extrapolation of the results for the smallest source–detector separation in Fig. 1 suggests that advective RBC motion may potentially dominate the laser speckle flowmetry signal, especially for larger vessels, such as the ones considered by Kazmi et al.[24]

6 Conclusion

We have presented a set of theoretical derivations for DCS measurements that take into account both diffusive and correlated advective scatterer motion and obtained results in agreement with our previous MC simulation study. We also provide expressions for considering realistic vascular morphologies and flow profiles and for linking DCS measured motion parameters with actual blood flow. Finally, we provide expressions for the correlation transfer equation and correlation diffusion equation in this context. These general equations may be used to model DCS measurements in the more complex, realistic configurations of tissue, optical sources, and detectors, as well as the realistic distributions of both morphological parameters and blood flow in vascular segments.

Disclosures

No conflicts of interest, financial or otherwise, are declared by the authors.

Acknowledgments

We would like to express our gratitude for support from the National Institutes of Health under Grants Nos. NS091230, EB015896, and CA187595.

References

1. D. Boas and A. Yodh, "Spatially varying dynamical properties of turbid media probed with diffusing temporal light correlation," *J. Opt. Soc. Am. A.* **14**(1), 192–215 (1997).
2. D. Boas, L. Campbell, and A. Yodh, "Scattering and imaging with diffusing temporal field correlations," *Phys. Rev. Lett.* **75**, 1855–1858 (1995).
3. S. A. Carp et al., "Validation of diffuse correlation spectroscopy measurements of rodent cerebral blood flow with simultaneous arterial spin

labeling MRI; towards MRI-optical continuous cerebral metabolic monitoring," *Biomed. Opt. Express* **1**, 553–565 (2010).
4. G. Yu et al., "Validation of diffuse correlation spectroscopy for muscle blood flow with concurrent arterial spin labeled perfusion MRI," *Opt. Express* **15**, 1064–1075 (2007).
5. E. M. Buckley et al., "Validation of diffuse correlation spectroscopic measurement of cerebral blood flow using phase-encoded velocity mapping magnetic resonance imaging," *J. Biomed. Opt.* **17**(3), 037007 (2012).
6. T. Durduran et al., "Optical measurement of cerebral hemodynamics and oxygen metabolism in neonates with congenital heart defects," *J. Biomed. Opt.* **15**(3), 037004 (2010).
7. E. M. Buckley et al., "Cerebral hemodynamics in preterm infants during positional intervention measured with diffuse correlation spectroscopy and transcranial Doppler ultrasound," *Opt. Express* **17**, 12571–12581 (2009).
8. N. Roche-Labarbe et al., "Noninvasive optical measures of CBV, StO_2, CBF index, and $rCMRO_2$ in human premature neonates' brains in the first six weeks of life," *Hum. Brain Mapp.* **31**(3), 341–352 (2010).
9. M. Kim et al., "Noninvasive measurement of cerebral blood flow and blood oxygenation using near-infrared and diffuse correlation spectroscopies in critically brain-injured adults," *Neurocrit. Care* **12**, 173–180 (2010).
10. C. Zhou et al., "Diffuse optical monitoring of hemodynamic changes in piglet brain with closed head injury," *J. Biomed. Opt.* **14**(3), 034015 (2009).
11. T. Durduran et al., "Diffuse optics for tissue monitoring and tomography," *Rep. Prog. Phys.* **73**(7), 076701 (2010).
12. S. A. Carp et al., "Due to intravascular multiple sequential scattering, diffuse correlation spectroscopy of tissue primarily measures relative red blood cell motion within vessels," *Biomed. Opt. Express* **2**, 2047–2054 (2011).
13. M. Ninck, M. Untenberger, and T. Gisler, "Diffusing-wave spectroscopy with dynamic contrast variation: disentangling the effects of blood flow and extravascular tissue shearing on signals from deep tissue," *Biomed. Opt. Express* **1**, 1502–1513 (2010).
14. D. A. Boas et al., "Establishing the diffuse correlation spectroscopy signal relationship with blood flow," *Neurophotonics* **3**(3), 031412 (2016).
15. N. A. Clark, J. H. Lunacek, and G. B. Benedek, "A study of Brownian motion using light scattering," *Am. J. Phys* **38**(5), 575–585 (1970).
16. M. Meinke et al., "Empirical model functions to calculate hematocrit-dependent optical properties of human blood," *Appl. Opt.* **46**, 1742–1753 (2007).
17. S. Sakadžić and L. V. Wang, "Ultrasonic modulation of multiply scattered coherent light: an analytical model for anisotropically scattering media," *Phys. Rev. E* **66**, 026603 (2002).
18. L. Gagnon et al., "Modeling of cerebral oxygen transport based on in vivo microscopic imaging of microvascular network structure, blood flow, and oxygenation," *Front. Comput. Neurosci.* **10**, 82 (2016).
19. R. Dougherty et al., "Correlation transfer—development and application," *J. Quant. Spectrosc. Radiat. Transfer* **52**, 713–727 (1994).
20. A. Ishimaru, "Correlation-functions of a wave in a random distribution of stationary and moving scatterers," *Radio Sci.* **10**(1), 45–52 (1975).
21. S. Sakadžić and L. V. Wang, "Correlation transfer equation for ultrasound-modulated multiply scattered light," *Phys. Rev. E* **74**, 036618 (2006).
22. H. Goldsmith and J. Marlow, "Flow behavior of erythrocytes. II. Particle motions in concentrated suspensions of ghost cells," *J. Colloid Interface Sci.* **71**(2), 383–407 (1979).
23. H. M. Varma et al., "Speckle contrast optical tomography: a new method for deep tissue three-dimensional tomography of blood flow," *Biomed. Opt. Express* **5**, 1275–1289 (2014).
24. S. M. S. Kazmi et al., "Flux or speed? Examining speckle contrast imaging of vascular flows," *Biomed. Opt. Express* **6**, 2588–2608 (2015).

Biographies for the authors are not available.